Mathematical modelling of oscillating patterns for chronic autoimmune diseases

R. Della Marca[1,a)], M.P. Machado Ramos[2,b)], C. Ribeiro[2,c)], A.J. Soares[2,d)]

[1]Department of Mathematical, Physical and Computer Sciences,
University of Parma, Parma, Italy

[2]Centro de Matemática, Universidade do Minho, Portugal

[a)]rossella.dellamarca@unipr.it, [b)]mpr@math.uminho.pt,
[c)]cribeiro@math.uminho.pt, [d)]ajsoares@math.uminho.pt

(October 20, 2021)

Abstract

Many autoimmune diseases are chronic in nature, so that in general patients experience periods of recurrence and remission of the symptoms characterizing their specific autoimmune ailment. In order to describe this very important feature of autoimmunity, we construct a mathematical model of kinetic type describing the immune system cellular interactions in the context of autoimmunity exhibiting recurrent dynamics. The model equations constitute a non-linear system of integro-differential equations with quadratic terms that describe the interactions between self-antigen presenting cells, self-reactive T cells and immunosuppressive cells. We consider a constant input of self-antigen presenting cells, due to external environmental factors that are believed to trigger autoimmunity in people with predisposition for this condition. We also consider the natural death of all cell populations involved in our model, caused by their interaction with cells of the host environment. We derive the macroscopic analogue and show positivity and well-posedness of the solution, and then we study the equilibria of the corresponding dynamical system and their stability properties. By applying dynamical system theory, we prove that steady oscillations may arise due to the occurrence of a Hopf bifurcation. We perform some numerical simulations for our model, and we observe a recurrent pattern in the solutions of both the kinetic description and its macroscopic analogue, which leads us to conclude that this model is able to capture the chronic behaviour of many autoimmune diseases.

Keywords: Mathematical biology. Kinetic theory. Autoimmune diseases. Cellular interactions. Dynamical systems. Hopf bifurcation.
AMS Subject Classification: 82C40, 92B05, 34A34, 37N25. 37G15.

1 Introduction

In the past, autoimmune diseases were considered to be rare, but rigorous epidemiological studies have shown that at present they affect around thirty five percent of the world population, with autoimmune thyroid disease and type I diabetes being the most common of these

conditions [24]. In fact, there are nearly one hundred distinct autoimmune diseases, some of them are organ-specific, such as primary biliary cirrhosis, and some others reflect a variety of immunological dysfunction involving multiple organs, such as systemic lupus [24].

Cells of the human immune system, called T lymphocytes (T cells), use special receptors on their surfaces to identify foreign antigens, such as bacteria and viruses. Usually, T cells that react to benign agents (self-antigens) are destroyed by the thymus. However, some of them survive this selective process and may be activated by a trigger. These cells are the self-reactive T cells (SRTCs), that produce cytokines after interaction with self-antigen presenting cells (SAPCs). An inflammatory cascade is then triggered, leading to damage to healthy tissue causing autoimmune disease. A combination of genetic predisposition and environmental factors contributes to the development of autoimmune diseases. In fact, there is growing evidence that environmental factors, such as exposure to infections, drugs, vaccines and chemicals, can constitute important triggers for the development of autoimmunity in susceptible people [21, 25]. Also, a diet rich in saturated fat, salt and containing pesticides and chemical additives is believed to have increasing prevalence in the diseases [17]. The mechanisms by which environmental factors can shape the immune system to generate autoimmunity include molecular mimicry, self-antigen modification, bystander activation, and immune reactivity modulation [21]. Most of these mechanisms lead to an increase in one way or another of the concentration of self-antigens in the human body.

An important characteristic of the adaptive immune response is the formation of immunological memory after initial antigen exposure that helps the immune system learn with experience. Naive T cells, upon antigen exposure, can generate T cell clones carrying the T cell receptor that recognize antigens most effectively and these are preserved in the form of long-lived memory T cells. On secondary antigen exposure, these expanded clones help mount a quicker and stronger immune response against invading pathogens.

Over the past decades, it has come to light that immunological memory can exist in the context of autoimmunity as well. It represents a constant-remembrance of self-antigen [8]. In fact, when memory T cells are formed against self-antigens they help mount a highly efficient pathogenic response against the body's own tissues. It is believed that these memory SRTCs may be responsible for the chronic nature of autoimmune diseases resulting in the relapse-remittance behaviour of these conditions. Memory T cells, by virtue of being long-lived, become very difficult to eliminate and therefore combating autoimmune memory has been a challenge not just in autoimmune diseases but also in transplantation, where the autoimmune memory cells attack the transplanted tissue.

All these issues regarding autoimmunity suggest very challenging mathematical problems at the level of modelling descriptions, rigorous analysis of the complex dynamics of the variables involved in autoimmunity and biological predictions based on numerical simulations.

There are some recent studies in mathematical modelling of autoimmune diseases and we quote here some of them. A macroscopic model is proposed in [27] and then revisited in [28, 29], where the theory of dynamical systems is applied to show that recurrent dynamics is observed in the solution due to a Hopf bifurcation. The authors investigate the existence of multiple limit cycles, backward bifurcations and turning points, in the context of autoimmunity and of other diseases. In paper [30], the authors construct a variant of the macroscopic model proposed in [27], that is simpler but retains the intrinsic dynamical behaviour of the original model, and investigate the influence of the effector-regulatory T cells in autoimmune diseases. Another interesting macroscopic model, whose solution reproduces a recurrence

behaviour, is proposed in [9], in view of describing relapsing-remitting stages in multiple sclerosis.

The aforementioned models [9,27–30] are all of macroscopic type, meaning that the mathematical framework consists of a system of ordinary differential equations that describe the global behaviour of the considered populations. The information on the individual activity of cells is not incorporated in these models, meaning that the description is given at a macroscopic scale.

However, it is well known that the cellular activity and the individual behaviour of cells affect the collective behaviour of its population and mathematical models developed at the cellular scale can capture these subtle effects. One possible approach to building a model at the cellular level comes from kinetic theory, in which the interactions among cells and the changes in their activity are incorporated in the dynamics. Another advantage of the kinetic approach is that, although models are developed at the cellular scale, suitable averaging processes and passage to the hydrodynamic limit allow to derive macroscopic equations describing the global behaviour of the populations. Therefore, the application of kinetic theory in the development of models of cellular interaction is an appropriate tool for making the connection between the individual behaviour, at the cellular level, and the collective behaviour, at a macroscopic scale.

A mathematical model of kinetic type is proposed in [13] and then reformulated in [12], in view of developing some numerical simulations able to describe typical dynamics of autoimmune diseases. Such papers do not exploit the interplay between the kinetic description and its corresponding macroscopic analogue but they are able to reproduce interesting numerical results describing typical behaviour of various autoimmune conditions, in particular absence of disease, mild symptoms and chronic disease.

Motivated by previous modelling descriptions of biological systems that are based on kinetic theory, such as those presented, for example, in papers [2, 3, 5, 7, 11], in Ramos *et al.* [14] a mathematical model of kinetic type describing the immune system interactions, in the context of autoimmune disease, is developed. The interacting populations are self-antigen presenting cells, self reactive T cells and the set of immunosuppressive cells (ISCs) consisting of regulatory T cells (Tregs) and Natural Killer cells (NKCs), that are believed to be important mediators within the immune system [1, 18, 22, 23]. In this work, the authors model the cellular dynamics when an autoimmune episode occurs, and do not describe the relapse-remittance behaviour of the autoimmune pathology. Consequently, the corresponding macroscopic description of the time evolution of the number of cells of each population in the aftermath of an autoimmune reaction does not model the relapse-remittance behaviour of the disease.

In the present paper, we construct a kinetic model exhibiting recurrent behaviour at the cellular scale, by introducing in the dynamics both a constant input of SAPCs, that is due to external environmental factors, and a natural death of all cells involved, caused by their interaction with cells of the host environment. The macroscopic model obtained from the kinetic system shows very rich dynamics. Choosing a proper bifurcation parameter, we are able to identify Hopf bifurcation critical points of the dynamical system, showing that the model may capture the recurrent dynamics characteristic of many autoimmune diseases, also at the macroscopic scale. Moreover, the macroscopic model presents consistency in terms of the mathematical properties that are necessary to support the numerical simulations developed in the work. The model developed here makes a bridge between the individual behaviour of

the cells and the collective behaviour of the corresponding populations. Moreover, it is such that the basic information on the kinetic model is contained in the corresponding macroscopic model, so that the mathematical properties of the macroscopic model and, in particular, the recurrent dynamics is also observed at the cellular level.

The mathematical framework of the model is described in Section 2, where both microscopic and macroscopic formulations are given. The positivity and well-posedness of the solution are also proven. We then study, in Section 3, the dynamical properties of the macroscopic system by determining its equilibria, analysing their local stability and identifying Hopf bifurcation critical points of the dynamical system. In Section 4, we perform numerical simulations of the macroscopic system and give a rather complete interpretation of the results in terms of both the analytical predictions and the biological considerations described above. Finally, in Section 5, we perform numerical simulations for the kinetic system. From these ones, we conclude that for certain values of the conservative parameters, the recurrent pattern observed at the macroscopic level is also present at the cellular level.

2 The mathematical framework

In this section, we propose a mathematical model capable of capturing the relapse-remission pattern typical of many autoimmune diseases due to their chronic nature [20].

We consider four interacting populations of the biological system that are believed to be important players in the autoimmune process, namely

- the A-population of self-antigen presenting cells (SAPCs),
- the R-population of self-reactive T cells (SRTCs),
- the S-population of immunosuppressive cells (ISCs),
- the H-population of cells of the host environment (HCs).

We use the indexes $i = 1, 2, 3, 4$ for the populations A, R, S and H, respectively.

We introduce first the system of evolution equations derived at the kinetic level for the distribution functions associated to the cell populations. This system describes the microscopic dynamics at the cellular level. Then, we derive the corresponding macroscopic system that consists in the balance laws describing the evolution of the global cell population densities.

The model derived here, with both kinetic and macroscopic counterparts, appears, in some sense, as a natural continuation of previous works by the authors, see [14] and [6], in view of implementing new and more relevant effects in the dynamics of the model, that are crucial for describing the recurrent behaviour of autoimmunity.

2.1 The microscopic model description

We introduce the distribution functions $f_i(t, u)$, $i = 1, 2, 3, 4$, associated to the populations considered here, such that $f_i(t, u)$ denotes the number of cells of the population i with activity $u \in [0, 1]$ at time $t \geq 0$.

The biological activity $u \in [0, 1]$ describes the functional state of each cell population A, R, S and H and is defined as follows.

- For the A-population, the activity variable u measures the ability to stimulate and activate the SRTCs.
- For the R-population, the activity variable u measures the quantity of cytokines secreted by SRTCs.
- For the S-population, the activity variable u measures the ability to inhibit the autoimmune response by either suppressing the activity of SAPCs and SRTCs, or eliminating SAPCs and SRTCs.
- For the H-population, the activity variable u describes the role of these cells in the apoptosis of SAPCs, SRTCs and ISCs.

We assume that the S-population is homogeneous with respect to its biological activity, so that the corresponding distribution function is independent of its functional state, i.e. $f_3 = f_3(t)$. We also assume that the cells of the H-population of the host environment exist in a huge amount, when compared with the other populations. As a consequence, we take the distribution function associated to the H-population to be constant, so that it does not appear explicitly in the model equations.

Moreover, we consider that all effective interactions in our model occur between a pair of cells and that they are instantaneous and homogeneous in space. The admissible interactions are of proliferative, destructive or conservative type and are the following.

- Proliferative interactions between SAPCs and SRTCs which increase the number of cells of both populations A and R with constant proliferative rates p_{12} and p_{21}, respectively.
- Conservative interactions between SAPCs and SRTCs which increase the activity of cells of both populations A and R at constant conservative rates c_{12} and c_{21}, respectively, while maintaining the number of cells of both populations.
- Proliferative interactions between SAPCs and ISCs which increase the number of cells of population S with a constant proliferative rate p_{31}.
- Destructive interactions between SAPCs and ISCs which decrease the number of cells of population A with a constant destructive rate d_{13}.
- Conservative interactions between SAPCs and ISCs which decrease the activity of population A at a constant conservative rate c_{13}, while maintaining the number of cells of both populations.
- Destructive interactions between SRTCs and ISCs which decrease the number of cells of population R with a constant destructive rate d_{23}.
- Conservative interactions between SRTCs and ISCs which decrease the activity of population R at a constant conservative rate c_{23}, while maintaining the number of cells of both populations.
- Destructive interactions between SAPCs, SRTCs, ISCs and host environment cells which decrease the A, R and S cell numbers with constant death rates d_1, d_2 and d_3, respectively.

All proliferative interactions are such that the cloned cells inherit the same aggressive state as their mother cells.

Finally, we consider a source term α representing a constant input of SAPCs, due to the effect of certain environmental factors, such as exposure to infections, drugs, vaccines and chemicals as well as due to unhealthy dietary habits. These factors are believed to trigger mechanisms that lead to the development of autoimmunity, by causing the increase, in direct or indirect way, of the concentration of self-antigens in the human body [21].

The evolution equations for the distribution functions f_i, $i = 1, 2, 3$, are derived, as usual, as evolution equations giving the time derivative of f_i in terms of the interaction operators describing all conservative, proliferative or destructive cellular interactions [4]. These interaction operators, with the addition of natural death terms and the constant input source α, are derived in a similar way to that explained in [14], so we omit the details here. The system so obtained consists of the following three coupled integro-differential equations

$$\begin{aligned}
\partial_t f_1(t,u) =& \alpha + 2c_{12}\int_0^u (u-v) f_1(t,v)\mathrm{d}v \int_0^1 f_2(t,w)\mathrm{d}w - c_{12}(u-1)^2 f_1(t,u)\int_0^1 f_2(t,w)\mathrm{d}w \\
&+ 2c_{13} f_3(t)\int_u^1 (v-u) f_1(t,v)\mathrm{d}v - c_{13}u^2 f_1(t,u) f_3(t) \\
&+ p_{12} f_1(t,u)\int_0^1 f_2(t,w)\mathrm{d}w - d_{13} f_1(t,u) f_3(t) - d_1 f_1(t,u), \\
\partial_t f_2(t,u) =& 2c_{21}\int_0^u (u-v) f_2(t,v)\mathrm{d}v \int_{w^*}^1 f_1(t,w)\mathrm{d}w - c_{21}(u-1)^2 f_2(t,u)\int_{w^*}^1 f_1(t,w)\mathrm{d}w \\
&+ 2c_{23} f_3(t)\int_u^1 (v-u) f_2(t,v)\mathrm{d}v - c_{23}u^2 f_2(t,u) f_3(t) \\
&+ p_{21} f_2(t,u)\int_0^1 f_1(t,w)\mathrm{d}w - d_{23} f_2(t,u) f_3(t) - d_2 f_2(t,u), \\
\dot{f}_3(t) =& p_{31} f_3(t)\int_0^1 f_1(t,w)\mathrm{d}w - d_3 f_3(t),
\end{aligned} \tag{1}$$

for all $u \in [0,1]$ and all $t \geq 0$, the upper dot being used to denote the time derivative. Here, $w^* \in]0,1[$ denotes the immunological tolerance of SRTCs to SAPCs, in the sense that the greater the value of w^* the less efficient are SAPCs in increasing the activity of SRTCs after encounter. Note that the last term in each equation of system (1) describes the destructive interactions with the host environment cells. The distribution function f_4 associated to the H-population does not appear explicitly in these terms because it is assumed to be constant during the evolution. Therefore, we have rescaled the death rates and used the notation d_i, $i = 1, 2, 3$, for the products $d_i f_4$.

The initial conditions for the system (1) are given by

$$f_1(0,u) = f_1^0(u), \quad f_2(0,u) = f_2^0(u), \quad f_3(0) = f_3^0. \tag{2}$$

2.2 The macroscopic model description

The macroscopic balance equations can be easily derived from the kinetic system (1), once we have introduced the expected number of cells of each population, at time $t \geq 0$, as follows

$$A(t) = \int_0^1 f_1(t,u)\mathrm{d}u, \quad R(t) = \int_0^1 f_2(t,u)\mathrm{d}u, \quad S(t) = f_3(t). \tag{3}$$

Then, we formally integrate the kinetic system (1) over the biological activity variable $u \in [0,1]$, and obtain macroscopic balance equations describing the time evolution of functions $A(t)$, $R(t)$ and $S(t)$. Conservative interactions do not give any contribution to these balance equations, since they do not modify the number of cells of each population. Therefore, the evolution equations for the densities of populations A, R and S are given by the following non-linear coupled system of ODEs,

$$\dot{A}(t) = \alpha + p_{12}A(t)R(t) - d_{13}A(t)S(t) - d_1A(t), \tag{4a}$$

$$\dot{R}(t) = p_{21}R(t)A(t) - d_{23}R(t)S(t) - d_2R(t), \tag{4b}$$

$$\dot{S}(t) = p_{31}S(t)A(t) - d_3S(t). \tag{4c}$$

For this system, we consider the positive initial data

$$A(0) = A_0 > 0, \quad R(0) = R_0 > 0, \quad S(0) = S_0 > 0. \tag{5}$$

The recruitment term α and the natural death terms d_i, $i = 1,2,3$, introduced in the kinetic dynamics, appear in equal manner in the macroscopic system (4), since they are uniform with respect to the biological activity.

In the kinetic model described in the previous subsection, we have assumed that proliferative encounters are such that cloned cells inherit the same aggressive state as their mother cell, at a constant proliferation rate, and, moreover, that the destructive encounters occur at a constant destruction rate. Under these assumptions, the boundedness of the solution of the macroscopic system implies the boundedness of the solution of the kinetic system, as proved in [2] for a rather general class of models. Therefore, the boundedness of the solution of the macroscopic system (4) implies the boundedness of the solution of the kinetic system (1).

These results imply that relevant information on the solution of the kinetic system (1) can be extracted from the mathematical analysis of the macroscopic equations (4), which is much easier to perform. This motivates us to carry out, in the section that follows, a qualitative mathematical analysis of the macroscopic model (4).

2.3 The consistency properties

This subsection is devoted to the fundamental consistency properties of positivity and well-posedness of the solution to the Cauchy problem (4)-(5).

Lemma 1. *Let $(A(t), R(t), S(t))$ be a solution of the Cauchy problem (4)-(5) defined on the time interval $[0,T]$, with T such that $0 < T < \infty$. Then, $A(t) > 0$, $R(t) > 0$ and $S(t) > 0$ for all $t \in [0,T]$.*

Proof. We start by proving the positivity of $A(t)$. By contradiction, let $\bar{t}_1 \in]0, T]$ be the first time instant at which A vanishes. Then, $A(\bar{t}_1) = 0$ and, from (4a),

$$\dot{A}(t)\big|_{t=\bar{t}_1} = \alpha > 0.$$

However, since $A(0) > 0$, this statement contradicts our assumption. Therefore, $A(t) > 0$ for all $t \in [0, T]$ with $0 < T < \infty$.

By applying the same reasoning as in Lemma 4.1 of paper [14], we can prove the positivity of $R(t)$ and $S(t)$. □

We now prove the existence and uniqueness of a global solution to the Cauchy problem (4)-(5) for the case in which the condition $p_{21}/p_{31} < 1$ is satisfied and the solution of the system does not blow-up. From a biological point of view, this condition corresponds to assuming that the proliferation of SRTCs, resulting from their encounter with SAPCs, occurs at a higher rate than that of the proliferation of ISCs, resulting from their encounter with SAPCs. The behaviour of the solution to system (4) is very sensitive to the value of the ratio p_{21}/p_{31}, in such a way that it may blow-up when $p_{21}/p_{31} \geq 1$. See paper [2] for a similar and more detailed analysis in the context of a model for a tumor-host dynamics.

Theorem 2. *Let us assume that the proliferative rates p_{21} and p_{31} are such that $p_{21} < p_{31}$. Then, the Cauchy problem (4)-(5) has a unique solution $(A(t), R(t), S(t))$ defined on all $\mathbb{R}_+$.*

Proof. Similarly to what is done in the proof of Theorem 4.1 in paper [14], we show that

$$R(t) \leq CS^{\lambda}(t)e^{\lambda d_3 t}, \qquad \text{with} \quad C = \frac{R(0)}{S^{\lambda}(0)}, \tag{6}$$

and $0 < \lambda < 1$ being such that $p_{21} = \lambda p_{31}$.

Using inequality (6) and the evolution equation (4a), we can easily prove that

$$\dot{A}(t) \leq \alpha + \frac{p_{12}}{p_{31}} Ce^{\lambda d_3 t} \left(\frac{\dot{S}(t)}{S(t)} + d_3 \right) S^{\lambda}(t). \tag{7}$$

Now, denoting by $g(t)$ the right-hand side of inequality (7) and evaluating its derivative $\dot{g}(t)$ at values of t where $g(t) = 0$, we obtain the following inequality

$$\dot{g}(t) \leq -\alpha\lambda p_{31} A(t) + \alpha \frac{\dot{S}(t)}{S(t)}, \tag{8}$$

where we have also used the evolution equation (4c). If we look at the expression on the right-hand side of inequality (8), we can easily conclude that this expression is always negative, since we have $\dot{S}(t) < 0$ when $g(t) = 0$. In the same way as in [14], we can then conclude that $A(t)$ is bounded and therefore, from equations (4b)-(4c), so are $R(t)$ and $S(t)$. □

The results stated in Lemma 1 and Theorem 2 assure the mathematical consistency of the model for what concerns the existence of solutions that are biologically significant. Therefore, they constitute a fundamental support to the numerical simulations for system (4). Also, they are essential to the study of the equilibria of this system and their stability.

3 Stability analysis

In this section, we proceed with the study of the dynamical system (4) and we investigate its ability to reproduce the recurrent behaviour of autoimmunity. More precisely, we determine the conditions for a Hopf bifurcation to occur, when an equilibrium loses its stability and a periodic solution arises [10, 19].

We restrict our search for equilibria to the set of biologically significant solutions to the Cauchy problem (4)-(5), namely solutions with all non-negative components, say

$$\mathcal{D} = \left\{ (A(t), R(t), S(t)) \in \mathbb{R}^3 : \, A(t) \geq 0, \, R(t) \geq 0, \, S(t) \geq 0 \right\}. \tag{9}$$

Furthermore, we choose the constant input of SAPCs, α, as bifurcation parameter.

3.1 Equilibria existence

We start by determining the equilibria of system (4) in the set $\mathcal{D}$. One can easily verify that the following Lemma holds.

Lemma 3. *System (4) admits three boundary steady-states in the set (9), namely an equilibrium with both self-reactive T cells and immunosuppressive cells equal to zero,*

$$E_1 = \left(\frac{\alpha}{d_1}, 0, 0 \right); \tag{10}$$

an equilibrium with no immunosuppressive cells,

$$E_2 = \left(\frac{d_2}{p_{21}}, \frac{d_1 d_2 - p_{21}\alpha}{d_2 p_{12}}, 0 \right), \tag{11}$$

that exists if $\alpha < \tilde{\alpha}$, with

$$\tilde{\alpha} = \frac{d_1 d_2}{p_{21}}; \tag{12}$$

and an equilibrium with no self-reactive T cells,

$$E_3 = \left(\frac{d_3}{p_{31}}, 0, \frac{-d_1 d_3 + p_{31}\alpha}{d_3 d_{13}} \right), \tag{13}$$

that exists if $\alpha > \bar{\alpha}$, with

$$\bar{\alpha} = \frac{d_1 d_3}{p_{31}}. \tag{14}$$

As far as the steady-states internal to $\mathcal{D}$ are concerned, system (4) admits a unique interior equilibrium,

$$E_4 = \left(\frac{d_3}{p_{31}}, \frac{d_3 d_{13}(d_3 p_{21} - d_2 p_{31}) + d_{23} p_{31}(d_1 d_3 - p_{31}\alpha)}{d_3 d_{23} p_{12} p_{31}}, \frac{d_3 p_{21} - d_2 p_{31}}{d_{23} p_{31}} \right), \tag{15}$$

that exists if both $s_4 > 0$ and $\alpha < \alpha^*$, with

$$s_4 = d_3 p_{21} - d_2 p_{31}, \tag{16a}$$

$$\alpha^* = \frac{d_3 d_{13} s_4}{d_{23} p_{31}^2} + \bar{\alpha}, \tag{16b}$$

and $\bar{\alpha}$ as given in (14).

Proof. The determination of equilibria E_1, E_2, E_3 and E_4 easily follows by setting the right-hand side of system (4) equal to zero and calculating the corresponding solutions. Equilibria existence conditions are obtained by requiring the non-negativity of their components and solving, when possible, in terms of the bifurcation parameter α. □

Note that E_4 is the unique "biologically-meaningful" equilibrium in the context of our model, because E_1, E_2 and E_3 predict the extinction of at least one of the interacting populations.

3.2 Equilibria stability

We now proceed to analyse the stability of the equilibria. The results of this analysis are summarized in the following theorem.

Theorem 4. *Let us consider the equilibria of system (4), E_i, $i = 1, \ldots, 4$. We assume that they belong to the set $\mathcal{D}$ defined in (9), see Lemma 3. Let $\tilde{\alpha}$, $\bar{\alpha}$, s_4, α^* be the quantities defined in (12)-(14)-(16a)-(16b), respectively. Then,*

(i) *E_1 is unstable if $\alpha > \tilde{\alpha}$ or $\alpha > \bar{\alpha}$. Otherwise, if $\alpha < \min\{\tilde{\alpha}, \bar{\alpha}\}$, it is locally asymptotically stable (LAS).*

(ii) *E_2 is unstable.*

(iii) *E_3 is unstable if $\alpha < \alpha^*$. Otherwise, if $\alpha > \alpha^*$, it is LAS.*

(iv) *E_4 is unstable if*

$$\alpha < \alpha^* - \frac{d_3 d_{13} s_4}{d_{23} p_{21} p_{31}}.$$

Otherwise, if

$$\alpha \geq \alpha^* - \frac{d_3 d_{13} s_4}{d_{23} p_{21} p_{31}},$$

there exists a positive value

$$\alpha^H \in \left]\alpha^* - \frac{d_3 d_{13} s_4}{d_{23} p_{21} p_{31}}, \alpha^*\right[$$

such that E_4 is unstable for

$$\alpha^* - \frac{d_3 d_{13} s_4}{d_{23} p_{21} p_{31}} \leq \alpha < \alpha^H,$$

whereas it is LAS for $\alpha^H < \alpha < \alpha^*$. In particular, Hopf bifurcations occur at $\alpha = \alpha^H$ and the bifurcating solution is periodic in time with period $T = 2\pi/\omega$ and frequency

$$\omega = \sqrt{\frac{d_3 s_4 (\alpha^* - \alpha^H)}{p_{31} \alpha^H}}.$$

Proof. The Jacobian of system (4) reads

$$J = \begin{pmatrix} p_{12}R - d_{13}S - d_1 & p_{12}A & -d_{13}A \\ p_{21}R & p_{21}A - d_{23}S - d_2 & -d_{23}R \\ p_{31}S & 0 & p_{31}A - d_3 \end{pmatrix}. \tag{17}$$

(i) The matrix (17) evaluated at the equilibrium E_1, given in (10), becomes

$$J(E_1) = \begin{pmatrix} -d_1 & \dfrac{p_{12}\alpha}{d_1} & -\dfrac{d_{13}\alpha}{d_1} \\ 0 & \dfrac{p_{21}(\alpha - \tilde{\alpha})}{d_1} & 0 \\ 0 & 0 & \dfrac{p_{31}(\alpha - \bar{\alpha})}{d_1} \end{pmatrix},$$

with $\tilde{\alpha}$, $\bar{\alpha}$ given in (12)-(14), respectively. The eigenvalues of $J(E_1)$ are the diagonal entries. Hence, E_1 is LAS if $\alpha < \min\{\tilde{\alpha}, \bar{\alpha}\}$. Otherwise, if $\alpha > \tilde{\alpha}$ or $\alpha > \bar{\alpha}$, it is unstable.

(ii) The matrix (17) evaluated at the equilibrium E_2, given in (11), becomes

$$J(E_2) = \begin{pmatrix} -\dfrac{p_{21}\alpha}{d_2} & \dfrac{d_2 p_{12}}{p_{21}} & -\dfrac{d_2 d_{13}}{p_{21}} \\ \dfrac{p_{21}^2(\tilde{\alpha} - \alpha)}{d_2 p_{12}} & 0 & -\dfrac{d_{23}p_{21}(\tilde{\alpha} - \alpha)}{d_2 p_{12}} \\ 0 & 0 & \dfrac{d_2 p_{31}}{p_{21}} - d_3 \end{pmatrix}.$$

One can immediately get the eigenvalue $\lambda_1(E_2) = d_2 p_{31}/p_{21} - d_3$, whereas the other two eigenvalues are determined by the submatrix

$$\tilde{J}(E_2) = \begin{pmatrix} -\dfrac{p_{21}\alpha}{d_2} & \dfrac{d_2 p_{12}}{p_{21}} \\ \dfrac{p_{21}^2(\tilde{\alpha} - \alpha)}{d_2 p_{12}} & 0 \end{pmatrix},$$

which has $\mathrm{tr}\left(\tilde{J}(E_2)\right) < 0$ and $\det\left(\tilde{J}(E_2)\right) < 0$, whenever E_2 exists, see Lemma 3. Thus, E_2 is an unstable equilibrium.

(iii) The matrix (17) evaluated at the equilibrium E_3, given in (13), becomes

$$J(E_3) = \begin{pmatrix} -\dfrac{p_{31}\alpha}{d_3} & \dfrac{d_3 p_{12}}{p_{31}} & -\dfrac{d_3 d_{13}}{p_{31}} \\ 0 & \dfrac{d_{23}p_{31}(\alpha^* - \alpha)}{d_3 d_{13}} & 0 \\ \dfrac{p_{31}^2(\alpha - \bar{\alpha})}{d_3 d_{13}} & 0 & 0 \end{pmatrix},$$

with α^* given in (16b). It is straightforward to get the eigenvalue

$$\lambda_1(E_3) = \frac{d_{23}p_{31}(\alpha^* - \alpha)}{d_3 d_{13}},$$

whereas the other two eigenvalues are determined by the submatrix

$$\tilde{J}(E_3) = \begin{pmatrix} -\dfrac{p_{31}\alpha}{d_3} & -\dfrac{d_3 d_{13}}{p_{31}} \\ \dfrac{p_{31}^2(\alpha-\bar{\alpha})}{d_3 d_{13}} & 0 \end{pmatrix},$$

which has $\mathrm{tr}\left(\tilde{J}(E_3)\right) < 0$ and $\det\left(\tilde{J}(E_3)\right) > 0$, whenever E_3 exists, see Lemma 3. Hence, E_3 is LAS if $\lambda_1(E_3) < 0$, i.e. if $\alpha > \alpha^*$. Otherwise, if $\alpha < \alpha^*$, it is unstable.

(iv) Finally, the matrix (17) evaluated at the equilibrium E_4, given in (15), becomes

$$J(E_4) = \begin{pmatrix} -\dfrac{p_{31}\alpha}{d_3} & \dfrac{d_3 p_{12}}{p_{31}} & -\dfrac{d_3 d_{13}}{p_{31}} \\ \dfrac{p_{21}p_{31}(\alpha^*-\alpha)}{d_3 p_{12}} & 0 & -\dfrac{d_{23}p_{31}(\alpha^*-\alpha)}{d_3 p_{12}} \\ \dfrac{s_4}{d_{23}} & 0 & 0 \end{pmatrix}.$$

The characteristic polynomial of $J(E_4)$ is

$$p(\lambda) = \lambda^3 + a_2(\alpha)\lambda^2 + a_1(\alpha)\lambda + a_0(\alpha)$$

with

$$a_2(\alpha) = \frac{p_{31}\alpha}{d_3} > 0,$$

$$a_1(\alpha) = \frac{d_3 d_{13} s_4 - d_{23}p_{21}p_{31}\,(\alpha^*-\alpha)}{d_{23}p_{31}},$$

$$a_0(\alpha) = s_4\,(\alpha^*-\alpha) > 0,$$

and s_4 given in (16a), see existence conditions for E_4 in Lemma 3. By Descartes' rule of signs, it follows that E_4 is unstable if $a_1(\alpha) < 0$, i.e. if

$$\alpha < \alpha^* - \frac{d_3 d_{13} s_4}{d_{23}p_{21}p_{31}}.$$

Otherwise, if $a_1(\alpha) \geq 0$, then E_4 is LAS but can lose stability via a Hopf bifurcation [10, 19]. More precisely, according to the Routh-Hurwitz criterion, E_4 will be LAS if and only if $h(\alpha) = a_1(\alpha)a_2(\alpha) - a_0(\alpha)$ is positive, equivalently written as

$$h(\alpha) = \frac{\mathsf{A}\alpha^2 + \mathsf{B}\alpha + \mathsf{C}}{d_3 d_{23}} \tag{18}$$

with

$$\mathsf{A} = d_{23}p_{21}p_{31}, \quad \mathsf{B} = d_3 s_4(d_{13}+d_{23}) - d_{23}p_{21}p_{31}\alpha^*, \quad \mathsf{C} = -d_3 d_{23} s_4 \alpha^*.$$

Since $\mathsf{A} > 0$ and $\mathsf{C} < 0$, equation $h(\alpha) = 0$ has a unique positive solution, that we denote by α^H. Furthermore

$$h(\alpha^*) = \frac{d_{13}s_4\alpha^*}{d_{23}} > 0 > -\frac{d_3 d_{13} s_4^2}{d_{23}p_{21}p_{31}} = h\left(\alpha^* - \frac{d_3 d_{13} s_4}{d_{23}p_{21}p_{31}}\right),$$

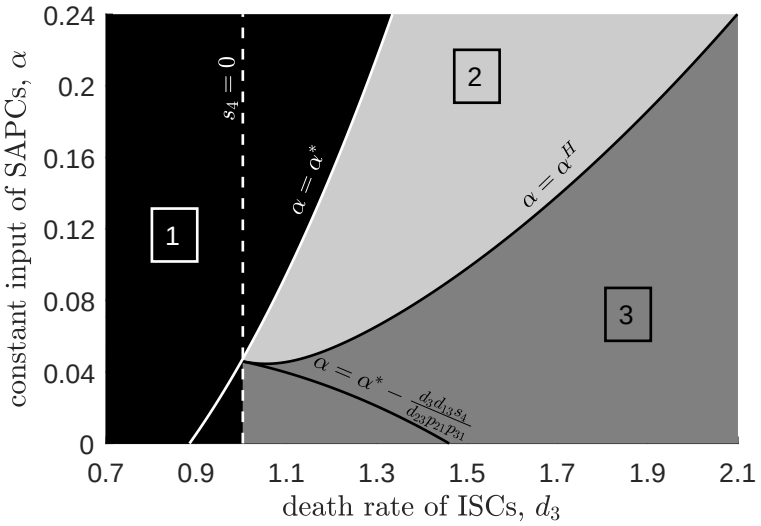

Figure 1: Bifurcation diagram for the equilibrium E_4 of system (4) in the parameter space (d_3, α). Region color is black (sector $\boxed{1}$) where E_4 does not exist, it is light grey (sector $\boxed{2}$) where E_4 is LAS and it is dark grey (sector $\boxed{3}$) where E_4 is unstable. Supercritical Hopf bifurcations occur at the points of the curve $\alpha = \alpha^H$. The other parameter values are specified in (21)-(22).

yielding

$$\alpha^* - \frac{d_3 d_{13} s_4}{d_{23} p_{21} p_{31}} < \alpha^H < \alpha^*.$$

Thus, E_4 is unstable for

$$\alpha^* - \frac{d_3 d_{13} s_4}{d_{23} p_{21} p_{31}} \leq \alpha < \alpha^H$$

and it is LAS for $\alpha^H < \alpha < \alpha^*$. At $\alpha = \alpha^H$ the test for non zero speed is fulfilled [10], that is

$$\partial_\alpha h(\alpha)\big|_{\alpha=\alpha^H} = \sqrt{\mathsf{B}^2 - 4\mathsf{AC}} \neq 0,$$

implying that a Hopf bifurcation occurs for $\alpha = \alpha^H$. The bifurcating solution is time-periodic with period $T = 2\pi/\omega$ and frequency $\omega = \sqrt{a_1(\alpha^H)} = \sqrt{a_0(\alpha^H)/a_2(\alpha^H)}$, see [19].

□

We note that in the above analysis we have chosen α as the bifurcation parameter since our intention is to study the effect of external environmental factors on the evolution of an autoimmune disease.

The results on existence and stability of the equilibrium E_4 presented in Lemma 3 and Theorem 4 are illustrated in Figures 1 and 2.

In Figure 1, we consider the parameter space (d_3, α), namely the pairs of the ISCs death rate, d_3, and the bifurcation parameter α, and depict the curves ruling the existence and

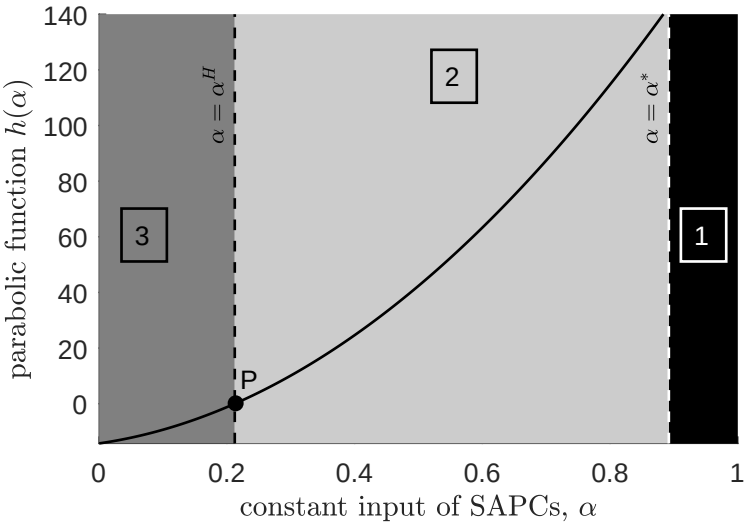

Figure 2: Representation of the parabolic function $h(\alpha)$, as given in (18), ruling the local stability properties of the equilibrium E_4 of system (4). Region color is black (sector $\boxed{1}$) where E_4 does not exist, light grey (sector $\boxed{2}$) where E_4 is LAS and it is dark grey (sector $\boxed{3}$) where E_4 is unstable. At point P, the function $h(\alpha)$ vanishes ($\alpha = \alpha^H$), and a supercritical Hopf bifurcation occurs. The other parameter values are specified in (21)-(22).

stability properties of E_4. All the other parameter values are set as in Section 4. The vertical line $s_4 = 0$ (i.e. $d_3 = d_2 p_{31}/p_{21}$) and the parabola $\alpha = \alpha^*$ are the thresholds for E_4 existence; the parabola

$$\alpha = \alpha^* - \frac{d_3 d_{13} s_4}{d_{23} p_{21} p_{31}} \tag{19}$$

separates the region where E_4 is always unstable from that where it can switch stability. In the latter the switch occurs in correspondence of the curve $\alpha = \alpha^H$, at which the system undergoes Hopf bifurcations. Specifically, periodic solutions exist on the underside of $\alpha = \alpha_H$ and are stable. Hence, the bifurcation is *supercritical*.

Figure 1 exhibits three sectors, labeled by $\boxed{1}$, $\boxed{2}$ and $\boxed{3}$. Sector $\boxed{1}$ in black corresponds to the region where the equilibrium E_4 does not exist; sector $\boxed{2}$ in light grey corresponds to the region where E_4 is LAS, whereas sector $\boxed{3}$ in dark grey corresponds to the region where E_4 is unstable. In particular, when $\alpha \approx]0, 0.045[$, E_4 is unstable whenever it exists; whereas for $\alpha > 0.045$ it can switch stability and passes from sector $\boxed{2}$ to sector $\boxed{3}$, or vice versa, by suitably varying the death rate d_3. We notice that, except for an initially slight decreasing shape, see $d_3 \approx]1.01, 1.06[$ in Figure 1, the curve of Hopf bifurcations locus $\alpha = \alpha^H$ is an increasing function of d_3. Namely, the higher is the ISCs death rate, d_3, or the smaller is the constant input of SAPCs, α, the lower are the chances of avoiding E_4 destabilization.

In Figure 2, we take $d_3 = 2$ and plot the values of the parabolic function $h(\alpha)$, defined in (18), by varying $\alpha \in [0, 1]$. As stated in proof of Theorem 4, this function rules the local stability properties of the equilibrium E_4. More precisely, for α values above the threshold (19), the stability of E_4 depends on the sign of $h(\alpha)$: it is LAS [resp. unstable] if $h(\alpha) > 0$ [resp. $h(\alpha) < 0$]. The function h vanishes at $\alpha = \alpha^H$, that is the locus of a Hopf bifurcation, see point P in Figure 2. In the diagram, we also depict the straight lines $\alpha = \alpha^H$ and $\alpha = \alpha^*$

that identify the three sectors, labeled by $\boxed{1}$, $\boxed{2}$ and $\boxed{3}$, for what concerns the existence and stability of the equilibrium E_4, that correspond to those sketched in Figure 1.

4 Numerical simulations: the macroscopic scenario

In this section we numerically solve model equations (4) in order to analyse the behaviour of the solutions that is predicted in the previous section. In accordance with Theorem 4, we show that, for suitable parameter values, long term periodic oscillations may take place. They can reasonably represent the recurrent behaviour of autoimmune diseases.

Numerical simulations are performed in Matlab [16]. We use the `ode45` solver for integrating the system and platform-integrated functions for getting the plots.

4.1 Input data

We assume the following initial data

$$(A_0, R_0, S_0) = (0.2,\ 0.015,\ 0.015), \tag{20}$$

which means an initial state of our biological system with equal number of cells for both R- and S-populations, of order 10^{-2}, and a larger number of cells of the A-population, of order 10^{-1}. From a biological point of view, this is justified by the fact that initially, before the immune system reacts wrongly to self-antigens, the number of both R and S cells is very low. This number increases significantly when they proliferate by encounters with A cells. In turn, A cells, being self elements of the human body, are initially more abundant in number.

We also set the following values for the proliferative and destructive rates

$$p_{12} = 0.07, \quad p_{21} = 16, \quad p_{31} = 20, \quad d_{13} = 0.35, \quad d_{23} = 0.035, \tag{21}$$

as well as for the natural death rates of the populations,

$$d_1 = 0.92, \quad d_2 = 0.8, \quad d_3 = 2. \tag{22}$$

Since it is difficult to get parameter estimations based on medical data found in specialized literature, we adopt a heuristic approach. Namely, parameter values are chosen on the basis of biological descriptions that appear favourable to the occurrence of the recurrent disease behaviour, associated to periods of relapse and remittance.

4.2 Results and discussion

The main objective of our numerical simulations is to capture the recurrence phenomena in autoimmunity. Therefore we perform some numerical tests with this idea in mind and vary the bifurcation parameter α in such a way that equilibrium E_4 of system (4) exists and is unstable, so that the desired oscillatory dynamics for the state variables $A(t)$, $R(t)$ and $S(t)$ will appear, as predicted by Lemma 3 and Theorem 4. This means that, with reference to

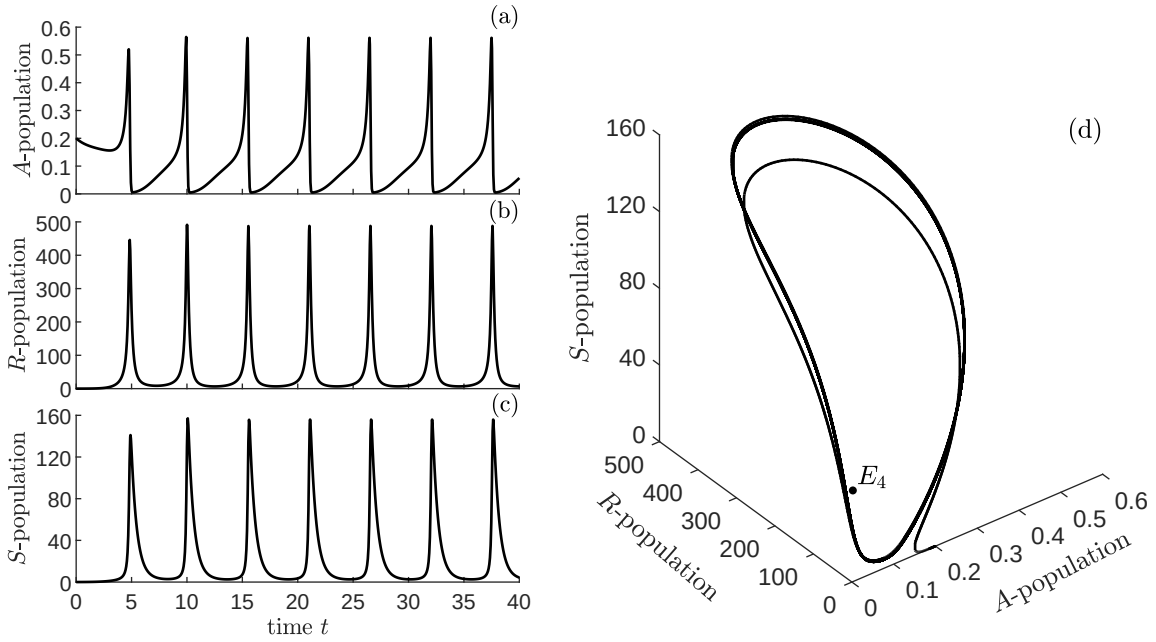

Figure 3: Numerical simulations of macroscopic model (4), by assuming $\alpha = 0.7\alpha^H$. Panel (a): dynamics of self-antigen presenting cells (A-population). Panel (b): dynamics of self-reactive T cells (R-population). Panel (c): dynamics of immunosuppressive cells (S-population). Panel (d): phase portrait of long term trajectory. The initial data and parameter values are specified in (20) and (21)-(22), respectively.

the bifurcation diagram in Figure 1, the simulations are performed by choosing the α values in sector $\boxed{3}$.

We consider different scenarios, in which the bifurcation parameter α varies from $\alpha = 0.7\alpha^H$ to $\alpha = 0.8\alpha^H$. The results are shown in Figures 3, 4, 5, where we represent, on the left, the temporal dynamics for the population densities $A(t)$, $R(t)$ and $S(t)$, see panels (a), (b) and (c), respectively, and, on the right, the phase portrait showing the long term trajectory of the solution of the dynamical system, see panels (d).

All simulations are performed with the initial data as given in (20) and input parameters for proliferative, destructive and natural death rates as given in (21) and (22).

Figures 3, 4, 5 clearly show the recurrence phenomena predicted by the results obtained in the previous section. We note that the R cell population proliferates significantly and we observe a lower proliferation of immunosuppressive cells represented by the S-population, implying that the S cells are unable to control the progression of the autoimmune reaction.

Furthermore, we can observe in Figures 3, 4, 5 that both maximum and minimum peaks occur around the same time instances for all populations. This is what we would expect, since all three cell populations are, in some sense, activated by one another during an attack by the immune system to self elements. So that, in the logic of the autoimmune reaction, when SAPCs start to decrease in number, after a certain maximum peak, there is no need for the immune system to generate more SRTCs to combat the pseudo effects of these self-antigens. In the same way, when SRTCs start to decrease in number, after a certain maximum peak, there is no need for the immune system to generate more ISCs to regulate the effect of the

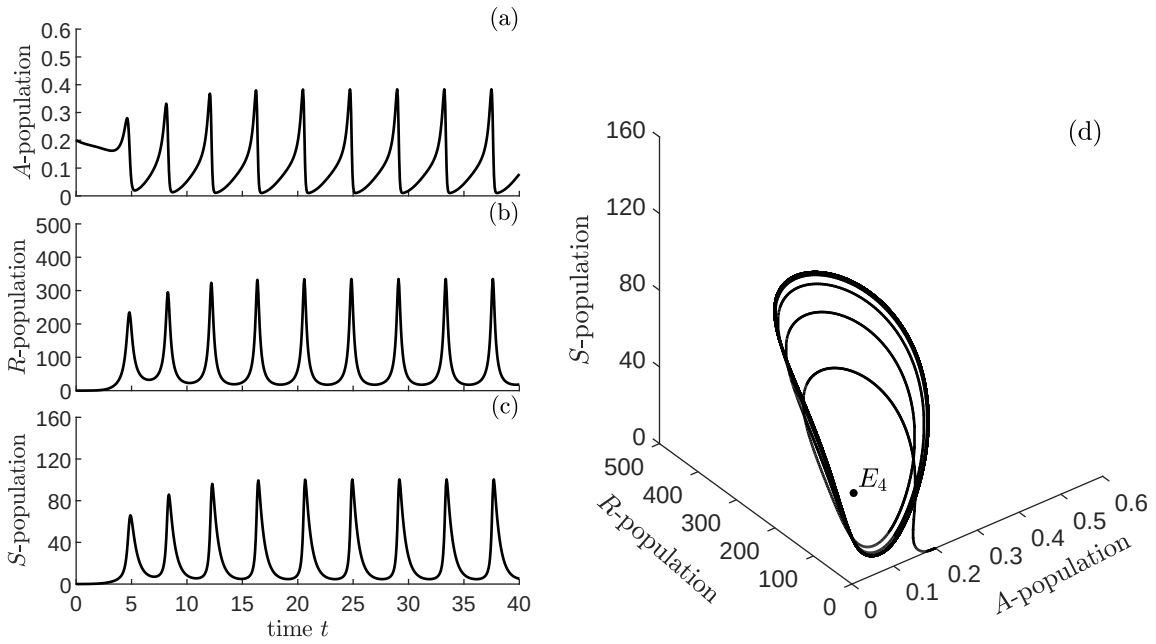

Figure 4: Numerical simulations of macroscopic model (4), by assuming $\alpha = 0.77\alpha^H$. Panel (a): dynamics of self-antigen presenting cells (A-population). Panel (b): dynamics of self-reactive T cells (R-population). Panel (c): dynamics of immunosuppressive cells (S-population). Panel (d): phase portrait of long term trajectory. The initial data and parameter values are specified in (20) and (21)-(22), respectively.

SRTCs.

When this recurrence behaviour occurs, we can say that patients suffer a relapse of their autoimmune disease, which in reality implies that they once again experience symptoms of their condition. After each peak, representing the relapse phase of the disease, we observe a decline in the number of cells of all populations involved in the process. This significant decrease of cells represents the remission phase of the autoimmune disease. The recurrence of the solution of system (4) observed in Figures 3, 4, 5 represents then the relapse-remission pattern that is typical of most autoimmune diseases.

When the bifurcation parameter α increases and we move from one diagram to another through Figures 3, 4, 5, the qualitative behaviour is similar both for the temporal dynamics of the population densities and for the phase portraits. However, we can observe that the initial transient period of the solution, before surrounding the limit cycle, increases when α approaches α^H. On the contrary, both the amplitude and the period of the long term oscillations reduce by increasing α towards α^H.

We complete our simulations with a scenario, which is not biologically relevant for the purpose of capturing the recurrence dynamics of the model, but it serves as a proof-of-principle verification of the analytical results obtained in Subsection 3.2. More precisely, we consider the case in which the equilibrium E_4 of system (4) exists and is LAS, see Lemma 3 and Theorem 4. To this aim, we maintain all the parameter values except for α, that is we set the value of α above the threshold value α^H, namely $\alpha = 1.1\alpha^H$. With reference to the bifurcation diagram in Figure 1, the simulations are performed in sector $\boxed{2}$.

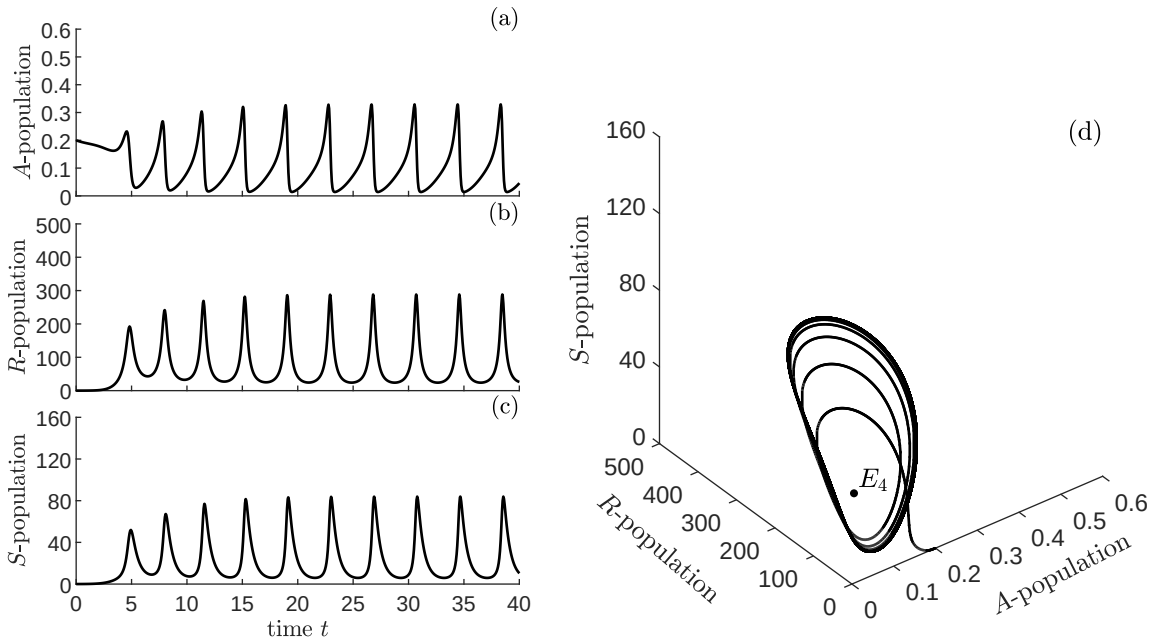

Figure 5: Numerical simulations of macroscopic model (4), by assuming $\alpha = 0.8\alpha^H$. Panel (a): dynamics of self-antigen presenting cells (A-population). Panel (b): dynamics of self-reactive T cells (R-population). Panel (c): dynamics of immunosuppressive cells (S-population). Panel (d): phase portrait of long term trajectory The initial data and parameter values are specified in (20) and (21)-(22), respectively.

Figure 6 presents the results obtained for this scenario. Panels (a), (b) and (c) show the evolution of the state variables $A(t)$, $R(t)$ and $S(t)$ towards their respective equilibrium values, and panel (d) shows the long term trajectory of the system asymptotically approaching the equilibrium E_4.

5 Numerical simulations: the microscopic scenario

We noted at the end of Subsection 2.2 that the qualitative behaviour of the solution of the kinetic system is similar in nature to that of its macroscopic counterpart. Therefore, the properties proved in Section 2.3 for the macroscopic system (4) are also valid for the kinetic system (1). Having this idea in mind, our aim in this subsection is to reproduce, at the kinetic level, recurrence patterns similar to those observed in Figures 3, 4, 5. In fact, we illustrate in what follows that, at least for certain values of the conservative rates appearing in the kinetic system, the recurrence patterns are also obtained at the cellular level.

We solve numerically the kinetic system (1), by discretizing the equations in the activation variable u and then using a trapezoidal quadrature rule to perform the numerical integration of the interaction terms. The numerical scheme is explained in detail in paper [14]. In the numerical simulations presented here, we take the following initial data

$$(f_1(0,u), f_2(0,u), f_3(0)) = (0.2,\, 0.015,\, 0.015), \qquad \text{for} \quad u \in [0,1], \tag{23}$$

and proliferation and destruction parameters given in (21) and (22), respectively. As for the

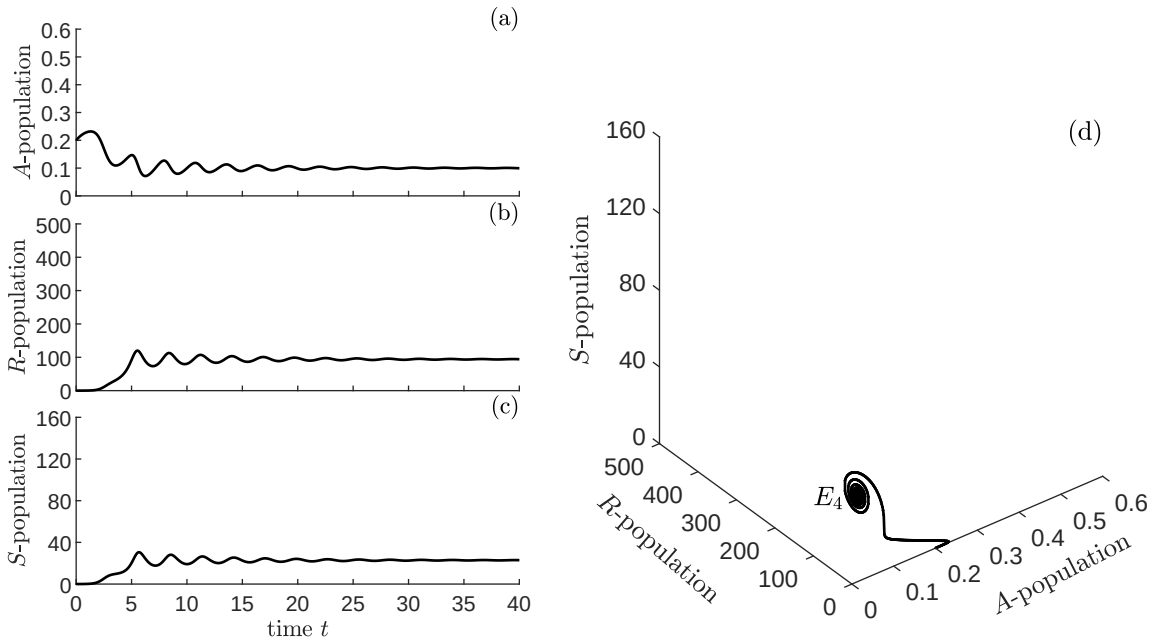

Figure 6: Numerical simulations of macroscopic model (4), by assuming $\alpha = 1.1\alpha^H$. Panel (a): dynamics of self-antigen presenting cells (A-population). Panel (b): dynamics of self-reactive T cells (R-population). Panel (c): dynamics of immunosuppressive cells (S-population). Panel (d): phase portrait of long term trajectory. The initial data and parameter values are specified in (20) and (21)-(22), respectively.

conservative terms appearing in this model, we consider

$$c_{12} = 20, \quad c_{13} = 0.07, \quad c_{21} = 0.035, \quad c_{23} = 16. \tag{24}$$

The kinetic system (1) is numerically solved by discretizing the equations with respect to the activation variable u and by employing the quadrature rule to approximate the integrals in the grid points. Proceeding in this way, we transform the integro-differential equations (1) into a larger system of nonlinear ODEs. The resulting nonlinear system of ODEs with initial conditions (2) is then numerically solved in Maple [15]. We use the Maple function dsolve with the option numeric that implements, by default, the Runge-Kutta-Fehberg method. See paper [14] for a detailed description of the numerical method.

The numerical simulations for the kinetic system are presented in Figures 7 and 8, for two different values of the recruitment term, namely for $\alpha = 0.77\alpha^H$ and $\alpha = 0.8\alpha^H$, respectively. The panels show similar recurrence patterns in the distribution functions f_i as those observed for the population densities in Figures 4 and 5, respectively. Comparing the profiles shown in Figures 4 and 7, we can acknowledge that the matching between the results obtained with the microscopic system and its macroscopic analogue is very good. In fact, we can see that both exhibit nine peaks with identical period occurring around the same time instances for all populations. Moreover, both maximum and minimum peaks of the distribution function observed in the profiles of Figure 7 occur around the same time instances

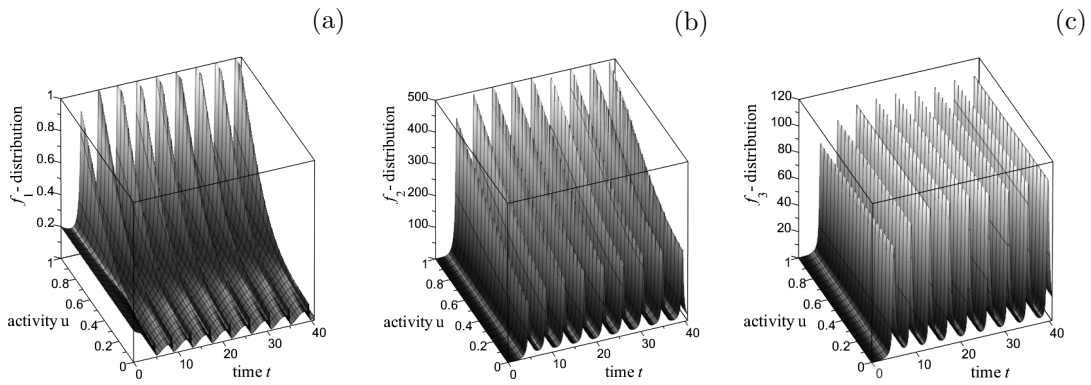

Figure 7: Numerical simulations of kinetic model (1), by assuming $\alpha = 0.77\alpha^H$. Panel (a): Cellular time-activity dynamics of self-antigen presenting cells (A-population). Panel (b): Cellular time-activity dynamics of self-reactive T cells (R-population). Panel (c): Cellular time-activity dynamics of immunosuppressive cells (S-population). The initial data and parameter values are specified in (23) and (21)-(22)-(24), respectively.

than the corresponding peaks for the densities of the respective populations observed in the profiles of Figure 4.

The same happens if we compare the profiles shown in Figures 5 and 8, both showing ten peaks. Also, both maximum and minimum peaks of the distribution function occur around the same time instances for all populations, in accordance to what can be observed for the densities of these populations in Figure 5. Once again, both maximum and minimum peaks of the distribution function observed in Figure 8 occur around the same time instances than the corresponding peaks for the densities of the respective populations in Figure 5.

We can also observe that the peaks for $f_1(t,u)$ and $f_2(t,u)$, shown in panels (a) and (b) of Figures 7 and 8, occur for high values of the activity, mainly due to the fact that in the simulations of the microscopic model we include considerably high values for the conservative terms, that are responsible for the increase in number of more active SAPCs and SRTCs. Also, the peaks for $f_1(t,u)$ and $f_2(t,u)$, shown in panels (a) and (b) of Figures 7 and 8 achieve higher values than those shown in Figures 4 and 5 for the corresponding macroscopic densities $A(t)$ and $R(t)$. This can be easily explained, since Figures 4 and 5 show an averaged behaviour with respect to the biological activity u, see the definitions (3).

6 Summary and perspectives

In this work, we establish a new kinetic model and derive its macroscopic counterpart, in order to describe the oscillating behaviour of the cellular dynamics involved in the development of chronic autoimmunity. This recurrent pattern is obtained by considering a recruitment term, α, representing a constant renewal of self-antigen presenting cells due to external environmental factors, along with a death term for each population, d_i, $i = 1, \ldots, 3$, representing the natural death of the cells caused by their interaction with the host environment.

We prove the existence and uniqueness of a global solution of our macroscopic system under a certain assumption on two of the proliferative parameters of the model, as well as

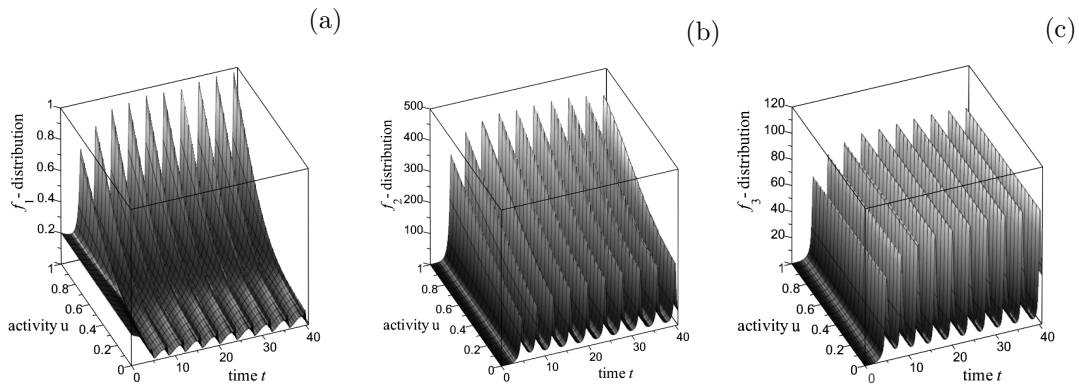

Figure 8: Numerical simulations of kinetic model (1), by assuming $\alpha = 0.8\alpha^H$. Panel (a): Cellular time-activity dynamics of self-antigen presenting cells (A-population). Panel (b): Cellular time-activity dynamics of self-reactive T cells (R-population). Panel (c): Cellular time-activity dynamics of immunosuppressive cells (S-population). The initial data and parameter values are specified in (23) and (21)-(22)-(24), respectively.

positivity of this solution in a general scenario.

We then study the dynamical properties of the macroscopic system and identify Hopf bifurcation critical points that lead to steady oscillations.

We perform numerical simulations for both the macroscopic and the kinetic systems and the results show recurrent behaviour of the solution, with repeated increase and decrease of the cellular densities of the populations involved in the process, at regular intervals of time. A significant increase of the cell numbers describes the relapse stage of the disease implying the flare up of the symptoms, while the decrease of these cell numbers represents the remission stage of the disease implying a relaxation or even disappearance of the symptoms. Based on the numerical results, the period of the oscillations observed in the numerical solution increases with the increasing of the bifurcation parameter α, indicating the possibility of determining certain subtypes of autoimmune diseases by the intrinsic value of its bifurcation parameter, related to the renewal of self-antigen presenting cells by external factors, and respective pattern of the recurrence behaviour, as already discussed in [26] and [27]. We also find that, for given parameter values, the chance of observing long term oscillating solutions is higher when the death rate of immunosuppressive cells, d_3, is higher, or when the constant input of self-antigen presenting cells, α, is smaller, see the bifurcation diagram in Figure 1.

We conclude that both the analytical and numerical outcome of our study suggests that the model developed in this work is able to describe not only the evolution in time of the cell populations that are believed to be the main players in the development of autoimmunity, but also the chronic nature of most autoimmune conditions.

Moreover, the model proposed here presents, in our opinion, some features that should be highlighted. One important aspect is that the individual cellular behaviour is incorporated in the kinetic dynamics and thus the model is able to describe the interactions among cells and the changes on their activity. At the same time, the macroscopic analogue derived from the kinetic system reflects the cellular behaviour on the global dynamical pattern of the populations and therefore allows us to relate both cellular and global performances.

This duality is an advantage over the macroscopic models studied in papers [9, 27–30] and [12, 13], where the individual behaviour of cells is not taken into account, and also over the kinetic models developed in [12, 13], where the relation to the macroscopic behaviour of the populations is not considered. Another very important aspect of our work is that, at variance with papers [13] and [27, 29], where the recurrent behaviour of the solution of the models is mainly due to the imbalance of the cells of the immune system, in our model we show that factors external to the immune system could produce, as well, recurrent dynamics in the model solution.

In future research, we plan, using clinical data, to consider different types of autoimmune diseases based on the recurrence pattern, and to investigate optimal therapies. This can be done by including, in the model developed here, a new variable representing a therapeutic procedure, and studying the impact of the therapy on the recurrent behaviour of the system solutions.

A more challenging problem that we plan to tackle in the future is the introduction of suitable memory terms in the kinetic model, so that, in practice, the interaction between pairs of cells may generate an output with a certain time delay generated by these memory terms.

Acknowledgments

This work is partially supported by the Portuguese FCT Projects UIDB/00013/2020 and UIDP/00013/2020 of CMAT-UM. Support by INdAM-GNFM and by University of Parma is also gratefully acknowledged by RDM.

References

[1] B. Akkaya, Y. Oya, M. Akkaya, J. Al Souz, A. H. Holstein, O. Kamenyeva, J. Kabat, R. Matsumura, D. W. Dorward, D. D. Glass, and E. M. Shevach. Regulatory T cells mediate specific suppression by depleting peptide–MHC class II from dendritic cells. *Nature Immunology*, 20(2):218–231, 2019.

[2] L. Arlotti and M. Lachowicz. Qualitative analysis of a nonlinear integrodifferential equation modeling tumor–host dynamics. *Mathematical and Computer Modelling*, 23(6):11–29, 1996.

[3] A. Bellouquid and E. de Angelis. From kinetic models of multicellular growing systems to macroscopic biological tissue models. *Nonlinear Analysis: Real World Applications*, 12(2):1111–1122, 2011.

[4] C. Cercignani. *The Boltzmann Equation and Its Applications*. Springer, New York, 1988.

[5] M. Conte, M. Groppi, and G. Spiga. Qualitative analysis of kinetic-based models for tumor-immune system interaction. *Discrete & Continuous Dynamical Systems - B*, 23(6):2393–2414, 2018.

[6] M. F. P. Costa, M. P. Machado Ramos, C. Ribeiro, and A. J. Soares. Optimal control model of immunotherapy for autoimmune diseases. *Mathematical Methods in the Applied Sciences*, 2021. DOI: 10.1002/mma.7318.

[7] M. Delitala, U. Dianzani, T. Lorenzi, and M. Melensi. A mathematical model for immune and autoimmune response mediated by T-cells. *Computers & Mathematics with Applications*, 66(6):1010–1023, 2013.

[8] P. Devarajan and Z. Chen. Autoimmune effector memory T cells: the bad and the good. *Immunologic Research*, 57(1-3):12–22, 2013.

[9] M. Elettrebya and E. Ahmedb. A simple mathematical model for relapsing-remitting multiple sclerosis (RRMS). *Medical Hypotheses*, 135:109478, 2020.

[10] J. Guckenheimer and P. Holmes. *Nonlinear Oscillations, Dynamical Systems, and Bifurcations of Vector Fields*. Springer, Berlin, 1983.

[11] M. Kolev. Mathematical modelling of the competition between tumors and immune system considering the role of the antibodies. *Mathematical and Computer Modelling*, 37(11):1143–1152, 2003.

[12] M. Kolev. Mathematical analysis of an autoimmune diseases model: Kinetic approach. *Mathematics*, 7(1024):1–14, 2019.

[13] M. Kolev and I. Nikolova. A mathematical model of some viral-induced autoimmune diseases. *Mathematica Applicanda*, 46(1):97–108, 2018.

[14] M. P. Machado Ramos, C. Ribeiro, and A. J. Soares. A kinetic model of T cell autoreactivity in autoimmune diseases. *Journal of Mathematical Biology*, 79(6):2005–2031, 2019.

[15] Maple. Maple release 2018.2. Maplesoft, a division of Waterloo Maple Inc., Waterloo, Ontario, 2018.

[16] MATLAB. Matlab release 2020a. The MathWorks, Inc., Natick, MA, 2020.

[17] I. Petta, J. Fraussen, V. Somers, and M. Kleinewietfeld. Interrelation of diet, gut microbiome, and autoantibody production. *Frontiers in Immunology*, 9:439, 2018.

[18] A. Poggi and M. R. Zocchi. NK cell autoreactivity and autoimmune diseases. *Frontiers in Immunology*, 5:27, 2014.

[19] S. Rionero. Hopf bifurcations in dynamical systems. *Ricerche di Matematica*, 68(2):811–840, 2019.

[20] M. D. Rosenblum, K. A. Remedios, and A. K. Abbas. Mechanisms of human autoimmunity. *The Journal of Clinical Investigation*, 125(6):2228–2233, 2015.

[21] C. Selmi, B. Gao, and M. E. Gershwin. The long and latent road to autoimmunity. *Cellular & Molecular Immunology*, 15(6):543–546, 2018.

[22] A. Sharabi, M. G. Tsokos, Y. Ding, T. R. Malek, D. Klatzmann, and G. C. Tsokos. Regulatory T cells in the treatment of disease. *Nature Reviews Drug Discovery*, 17(11):823–844, 2018.

[23] Z. Tian, M. E. Gershwin, and C. Zhang. Regulatory NK cells in autoimmune disease. *Journal of Autoimmunity*, 39(3):206–215, 2012.

[24] L. Wang, F.-S. Wang, and M. E. Gershwin. Human autoimmune diseases: a comprehensive update. *Journal of Internal Medicine*, 278(4):369–395, 2015.

[25] Z. Xiang, Y. Yang, C. Chang, and Q. Lu. The epigenetic mechanism for discordance of autoimmunity in monozygotic twins. *Journal of Autoimmunity*, 83:43–50, 2017.

[26] P. Yu and X. Wang. Analysis on recurrence behavior in oscillating networks of biologically relevant organic reactions. *Mathematical Biosciences and Engineering*, 16(5):5263–5286, 2019.

[27] W. Zhang, L. Wahl, and P. Yu. Modeling and analysis of recurrent autoimmune disease. *SIAM Journal on Applied Mathematics*, 74(6):1998–2025, 2014.

[28] W. Zhang, L. Wahl, and P. Yu. Backward bifurcations, turning points and rich dynamics in simple disease models. *Journal of Mathematical Biology*, 73:947–976, 2016.

[29] W. Zhang and P. Yu. Hopf and generalized hopf bifurcations in a recurrent autoimmune disease model. *International Journal of Bifurcation and Chaos*, 26(5):1650079, 2016.

[30] W. Zhang and P. Yu. Revealing the role of the effector-regulatory t cell loop on autoimmune disease symptoms via nonlinear analysis. *Communications in Nonlinear Science and Numerical Simulation*, 93:105529, 2021.